

## Full Length Article

# A transcriptomic approach for evaluating the relative potency and mechanism of action of azoles in the rat Whole Embryo Culture



Myrto Dimopoulou<sup>a,b,\*</sup>, Aart Verhoef<sup>b</sup>, Jeroen L.A. Pennings<sup>b</sup>, Bennard van Ravenzwaay<sup>a,d</sup>,  
Ivonne M.C.M. Rietjens<sup>a</sup>, Aldert H. Piersma<sup>b,c</sup>

<sup>a</sup> Wageningen University, Division of Toxicology, Stippeneng 4, 6708WE Wageningen, The Netherlands

<sup>b</sup> National Institute of Public Health and the Environment (RIVM), 3720BA Bilthoven, the Netherlands

<sup>c</sup> Institute for Risk Assessment Sciences (IRAS), Utrecht University, 3584CM Utrecht, the Netherlands

<sup>d</sup> BASF SE, Experimental Toxicology and Ecology, RB/T – Z470, 67056 Ludwigshafen, Germany

## ARTICLE INFO

## Keywords:

Whole embryo culture  
Toxicogenomics  
Embryonic development  
Azoles  
Retinoic acid  
Sterol biosynthesis

## ABSTRACT

We evaluated the effect of six azoles on embryonic development in the rat whole embryo culture (WEC). Using the total morphological scoring system (TMS), we calculated the ID<sub>10</sub> concentration (effective dose for 10% decrease in TMS). For evaluating gene specific responses, we combined previously and newly collected transcriptomics data of rat WEC exposed to a total of twelve azoles at their ID<sub>10</sub> for 4 h. Results revealed shared expressions responses in genes involved in the retinoic acid (RA) and sterol biosynthesis pathways, which are respectively representatives of developmental toxicity and targeted fungicidal action of the azoles. Azoles with more pronounced effects on the regulation of RA-associated genes were generally characterized as more potent embryotoxicants. Overall, compounds with strong sterol biosynthesis related responses and low RA related responses were considered as more favourable candidates, as they specifically regulated genes related to a desired target response. Among the identified sterol associated genes, we detected that methylsterol monooxygenase 1 (Msmo1) was more sensitively induced compared to Cyp51, a classical biomarker of this pathway. Therefore, we suggest that Msmo1 could be a better biomarker for screening the fungicidal value of azoles. In summary, we conclude that the embryonic regulation of RA and sterol metabolic pathways could be indicators for ranking azoles as embryotoxicants and determining their drug efficacy.

## 1. Introduction

Regulatory guidelines for the risk assessment of chemicals require relatively high numbers of experimental animals for reproductive and developmental toxicity testing (van der Jagt et al., 2004). To reduce, refine and replace the use of laboratory animals, a variety of alternative assays has been developed over the past decades, including simple cell-line assays, organ cultures or more complicated whole embryo culture techniques and organs-on-a chip (Augustine-Rauch et al., 2010; Piersma, 2006).

An advanced *in vitro* model that mimics *in vivo* organogenesis and embryonic development is the rat whole embryo culture (WEC) technique (Piersma, 2004; Robinson et al., 2012d). It is a widely used technique for screening embryotoxicants by monitoring both neurulation and organogenesis during gestational days (GD) 10 to 12 (New et al., 1976). A variety of morphological endpoints is combined in the Total Morphological Score (TMS) (Piersma, 2004). Applying the TMS in rat WEC, effects of chemicals on the embryonic growth and

development can be studied both qualitatively and quantitatively. WEC also enables the implementation of toxicogenomic-based approaches for mechanistic evaluation of the embryotoxic profile of xenobiotics. Gene signatures can predate and predict morphological consequences of toxic stimuli (Daston and Naciff 2010; Dimopoulou et al., 2017; Luijten et al., 2010; Robinson et al., 2012a, 2010). Furthermore, transcriptomics can be applied to identify biomarkers for detecting specific embryotoxic responses (Robinson et al., 2012a).

Azoles are antifungal agents for clinical and agricultural use. They have been designed to affect the Cyp51 enzyme, which catalyses the conversion of lanosterol to ergosterol on the fungal cell membrane, and leads to cell death when affected (Marotta and Tiboni, 2010). In mammalian systems, Cyp51 is less sensitive to azoles, but still critical for the sterol biosynthesis pathway. Moreover, azoles can induce many toxic responses in mammals by disturbing P450-mediated pathways and interfering with retinoic acid (RA) homeostasis (de Jong et al., 2011; Dimopoulou et al., 2017, 2016; Menegola et al., 2006). RA is crucial for maintaining balanced embryonic growth and differentiation,

\* Corresponding author at: Wageningen University, Division of Toxicology, P.O. Box 8000, 6708WE Wageningen, The Netherlands.  
E-mail address: [dimopoulou.myr@gmail.com](mailto:dimopoulou.myr@gmail.com) (M. Dimopoulou).

and *Cyp26a1* is its key regulatory metabolic enzyme, catalysing the first step in the degradation of RA, (Piersma et al., 2017; Tonk et al., 2015). Previous *in vivo* and *in vitro* studies suggest that when rat embryos were exposed to either RA or azoles, similar teratogenic outcomes were observed, including craniofacial and axial defects (Cunningham and Duester, 2015; Luijten et al., 2010; Piersma et al., 2017; Robinson et al., 2012c). Therefore, RA modulation may play a role in the developmental toxicity due to azole exposure.

In our previous study (Dimopoulou et al., 2017), we combined the WEC technique with transcriptomic analysis for determining the effects of six azoles. Gene expression signatures of embryos exposed to the six tested azoles suggested that a RA-associated gene set corresponded with the toxicological mode of action while a sterol biosynthesis-related gene set represented the fungicidal activity of the azole compounds. In the present study, we assessed the relative embryotoxic potencies of six additional compounds – three known and three novel azoles – by performing a global gene expression profiling of these azoles. Subsequently, the gene expression data of all twelve compounds were evaluated in one combined analysis, focussing on the RA and sterol biosynthesis pathways. We aimed to define biomarkers related to the aforementioned pathways, as promising molecular endpoints for classifying the desired fungicidal as well as the embryotoxic responses of azoles, and correlating the latter with available *in vivo* embryotoxicity data.

## 2. Materials and methods

### 2.1. Animal care

As described in our previous WEC studies (Dimopoulou et al., 2017, 2016), all the animal studies were approved and performed at the National Institute of Public Health and the Environment (RIVM) in concordance with European regulations. Wistar rats (HsdCpd:WU) (Harlan, The Netherlands) were housed at the RIVM Animal Care facility in a climate-controlled room with a 12 h light cycle (04:00–16:00 dark). Water and food were provided *ad libitum*. After acclimating for 2 weeks, virgin female rats were housed with male rats for a 3-h mating period (9:00–12:00, described as GD 0). Mated dams were afterwards individually housed. Rats were daily monitored for their general health condition during the period of the present study.

### 2.2. Rat whole embryo culture

Following previous studies (Dimopoulou et al., 2017, 2016; Luijten et al., 2010; Piersma 2004; Robinson et al., 2010), on GD 10, between 9:00 and 12:00 a.m., dams were euthanized by intracardiac injection of T61<sup>R</sup> (Intervet, The Netherlands). Rat embryos were immediately separated from the uterus. The peripheral trophoblastic cell zone and parietal yolk sac membrane were removed under the microscope leaving both the visceral yolk sac and ectoplacental cone intact. Embryos with 1–5 somites were further cultured, while only embryos with 2–4 somites were used for gene expression studies (Luijten et al., 2010). Embryos were separately cultured in flasks with 2 mL culture medium, containing 90% pregnant bovine serum and 10% rat serum (Biochrom, Berlin, Germany), diluted with 14% Hank's solution (Gibco) and supplemented with 1.6 mg/mL D-glucose and 75 µg/mL L-methionine (Sigma-Aldrich, Zwijndrecht, The Netherlands). The culture flasks were placed in rotating incubators, completely protected from light exposure and with stable internal temperature of 37.7 °C. A mixture of gas was supplied twice daily for 30 s, with increasing concentration of oxygen: on the first day (GD10) at 9:00 and 16:00 (5% O<sub>2</sub>, 5% CO<sub>2</sub>, 90% N<sub>2</sub>), on the second day (GD11) at 9:00 and 16:00 (20% O<sub>2</sub>, 5% CO<sub>2</sub>, 75% N<sub>2</sub>) and on the third day (GD12) at 9:00 (40% O<sub>2</sub>, 5% CO<sub>2</sub>, 55% N<sub>2</sub>).

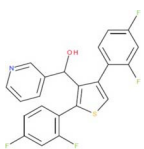
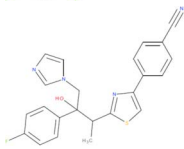
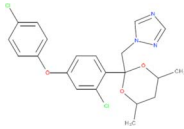
### 2.3. Morphological assessment and statistical analysis of individual endpoints

Embryos were cultured for 48 h (GD 10–12) and morphologically assessed according to the TMS system (Brown and Fabro, 1981). Twenty morphological endpoints were included in this morphological assessment, which were sub-divided into two basic groups. These represented growth parameters (including yolk sac diameter, crown-rump length, head diameter and number of somites) and developmental/functional parameters, such as yolk sac and allantoic blood circulation, heart formation and heart beating, embryo- turning, caudal neural tube, optic and otic system, fore- and hind- limb, branchial arches, mandibular and maxillary process and the shape and size of somites. The TMS is a quantitative system for identifying any possible specific and selective embryotoxic effect of the tested compounds in rat embryos. Therefore, the sum of scores for each of the morphological endpoints was calculated for detecting any morphological alteration and for comparing with the time-matched controls. Within each exposure group, including also the vehicle control (DMSO), 8 rat embryos were evaluated. For normalizing the data and eliminating daily variation, the GD10 embryos within the same exposure group were derived from dams sacrificed on different days. Statistical analysis was performed using the parametric (Student's *t*-test) and non-parametric (Mann-Whitney) (unpaired), two-sided, and with 95% confidence intervals. Due to high agreement between these approaches, the significance values deriving from the Student's *t*-test are shown here. Images of the examined embryos (exposed for 48 h to either DMSO or tested compounds) were obtained using an Olympus SZX9 camera at × 20 magnification and Olympus DP software.

### 2.4. Test compounds and exposure concentrations

This study combines data of six known azole compounds from our previous publication (Dimopoulou et al., 2017) and additional data of three known and three new azoles derived from the present study. For the present study, the following three known and three novel azoles were tested in rat WEC for 48 h (0–48 h) in a range of concentrations with the lowest concentration inducing no morphological effect to the highest being the maximal achievable concentration in culture. The three known azoles were: fenarimol (FEN; CAS#60168-88-9, purity 99.9%, Sigma-Aldrich, Zwijndrecht, The Netherlands); propiconazole (PRO; CAS#60207-90-1, purity 99.1%, Sigma-Aldrich, Zwijndrecht, The Netherlands); and tebuconazole (TEB; CAS#107534-96-3, purity 99.4%, Sigma-Aldrich, Zwijndrecht) at 20, 60 200 and 600 µM. BASF SE (Ludwigshafen, Germany) kindly provided the three novel azole-compounds (with purity > 95%) and their chemical information is summarised in Table 1. B595 and B600 were tested at 60, 200 and 600 µM; and B599 at 2, 6, 20 and 60 µM. All the compounds were dissolved in dimethyl sulfoxide (DMSO, Sigma-Aldrich, Zwijndrecht, The Netherlands), and all embryos were exposed to a final DMSO concentration of 0.1%. As has been previously described, 0.1% DMSO did not significantly alter the morphology (4 and 48 h) and has limited effects on gene expression after 4 h of exposure (Dimopoulou et al., 2017; Robinson et al., 2010). The concentration at which rat WEC were exposed to conduct the gene expression analysis was in the same line of concept with our previous study (Dimopoulou et al., 2017) and calculated after completing the morphological assessment of rat embryos (48 h). Next, we calculated the concentration which results to 10% reduction of the control TMS (ID<sub>10</sub>) with both PROAST (Slob, 2002) and Graphpad software ([www.graphpad.com](http://www.graphpad.com)). For microarray analysis, rat WEC were exposed for 4 h (0–4 h) to the tested compounds at their ID<sub>10</sub> values: FEN at 140 µM, PRO at 220 µM, TEB at 115 µM, B595 at 180 µM, B599 at 5 µM, and B600 at 110 µM, as derived from the concentration response curves on TMS.

**Table 1**  
Chemical information of the three novel azoles tested in the present study.

Code	Structure	Molecular weight (g/mol)
B595		415.4
B599		418.5
B600		434.3

## 2.5. Whole embryo RNA isolation

For transcriptomics, 4-h cultured embryos were quickly scored on the basis of their somite number, their position in the yolk sac, neural tube developmental stage, crown-rump length and head diameter. They were then isolated from the yolk sac and ectoplacental cone, placed in 200  $\mu$ L RNAlater (Ambion, Austin, Texas), stored for one week at 4 °C, and then stored for further processing at –80 °C. After the embryos were thawed on ice, they were separately homogenized by passing them 10 times through a 1 mL syringe with a 26G needle. RNA was further isolated by using the RNeasy Micro Plus RNA isolation kit (CAS number 74034, Qiagen, the Netherlands) and manufacturer's protocol. RNA was eluted with 14  $\mu$ M RNase-free H<sub>2</sub>O and stored at –80 °C. Quantity and quality of the isolated RNA were measured with Nanodrop (Nanodrop Technologies Inc., Wilmington, Delaware) and 2100 BioAnalyzer (Agilent Technologies, Palo Alto, California). Samples with absorbance value between 1.9 and 2.2 (ratio 260 nm/280 nm) and RNA integrity number (RIN) higher than 8 were further used for performing the microarray analysis.

## 2.6. Microarray hybridization

RNA hybridization and microarray experimentations were performed by the Dutch Service and Support Provider (MAD) of the University of Amsterdam, the Netherlands. In agreement with our previous publication (Dimopoulou et al., 2017), for every sample, RNA was amplified, biotin-labelled and hybridized to Affymetrix GeneChip HT RG-230 PM Array Plates according to the provided protocols by Affymetrix (Santa Clara, CA). After staining, the HT Array plate was read by the Affymetrix GeneChip® HT Scanner and analysed by the Affymetrix GeneChip® Operating Software. For performing the aforementioned steps, the GeneTitan® Hybridization, Wash, and Stain Kit for 3' IVT Arrays (cat no. 901530) was used. In total, 56 arrays were further analysed (8 embryos per exposure group, 6 tested compounds and 1 control group).

## 2.7. Microarray analysis and data processing

The quality control (QC) and the normalization of the microarray data were performed using the Affymetrix array QC pipeline at ArrayAnalysis.org webpage ([www.arrayanalysis.org](http://www.arrayanalysis.org)) (Eijssen et al., 2013), designed by the Department of Bioinformatics in Maastricht University. Due to normal expected biological differences between the two studies (Dimopoulou et al., 2017) and present) and, consequently, to eliminate any experimental-specific gene responses, the raw data

were separately normalized with their appropriate control for each study and accordingly processed. Raw microarray data were inspected for their quality by assessing the 3'/5' ratios for  $\beta$ -actin and GAPDH, RNA degradation, background intensity, signal quality and the probe-set homogeneity with NUSE (Normalized Unscaled Standard Error) and RLE (Relative Log Expression). The Affymetrix CEL files were further normalized by using the Robust Multichip Average (RMA) algorithm (Irizarry et al., 2003) and the Brainarray custom CDF version 19 probe set annotation (<http://brainarray.mbi.med.umich.edu/Brainarray/default.asp>) (Dai et al., 2005). In total, 13,877 probe sets, each corresponding to an Entrez Gene ID, were further evaluated by performing a statistical analysis in R ([www.R-project.org](http://www.R-project.org)) and Microsoft Excel. Raw and normalized data were deposited in NCBI GEO ([www.ncbi.nlm.nih.gov/geo/](http://www.ncbi.nlm.nih.gov/geo/)) under accession number GSE102082.

## 2.8. Identification of significantly altered genes

Normalized data were log transformed. For each exposure condition, gene expression data were compared to the appropriate control (each study has a separate control group), for calculating absolute average fold changes of individual gene expression. Differentially expressed genes were identified by using ANOVA, using a p-value < 0.001 and a False Discovery Rate (FDR) of 10%, as stringency criteria. The statistical criteria were set similar to earlier published studies from our laboratory, and they partly determined the number of genes differentially expressed. The 53 genes, which were differentially expressed in at least one of the eight rat WEC samples from their respective exposure groups, were combined for further analysis. Gene expression responses were visualized using a heatmap combined with hierarchical clustering (Euclidean distance, Ward linkage) as well as Principal Component Analysis (PCA). Each bar in the heatmap represents the average of the gene expression in the experimental group compared to the respective control group of each study.

## 2.9. Functional interpretation analysis of differentially expressed genes

Following the concept of our previous study (Dimopoulou et al., 2017), functional annotation and overrepresentation analysis were performed using DAVID (<https://david.ncifcrf.gov/>) (Huang da et al., 2009) and literature data (Robinson et al., 2012b,c; Tonk et al., 2015). Here, we additionally applied the gene sets already identified from our previous study, which included genes participating in RA pathway, general development and the sterol biosynthesis pathway. Furthermore, we indicated three additional pathways that importantly identified genes belong to apoptosis, neural differentiation, and vessel formation. The combined gene expression data were summarised to absolute average fold changes per pathway. Next, the absolute average fold changes of genes of interest or of the whole pathway per exposure group were plotted against the compound concentration used. Finally, the absolute fold change of gene expression per RA and sterol biosynthesis pathways versus the used ID<sub>10</sub> concentrations and the relative *in vivo* potencies of the tested compounds in rat embryos were plotted in a 3D plot using R.

## 2.10. In vivo data analysis

In addition to previously derived *in vivo* data (Dimopoulou et al., 2017), a literature overview was performed to determine the *in vivo* developmental toxic profile of the three known azoles. Applying the same criteria concerning the species, chemical exposure during specific GD and scheme of dosing range, we selected studies performed in rats orally exposed to the tested compounds during either GD6-15 or GD7-16 at multiple dose regimes. Studies with at least one control group and two dose groups were selected to allow analysis using the Benchmark Dose (BMD) approach. The BMD values were calculated based on the evidence of adverse skeletal changes or cleft palate formation, both

selected as sensitive endpoints of *in vivo* developmental toxicity and specific for the tested group of chemicals. For some of the tested compounds, other morphological endpoints were considered for calculating the BMD values, dependent on the specificity of the malformations observed. A concentration-response curve was fitted to the data to determine the BMD for the selected benchmark response (BMR) for each tested azole. The BMD was defined as 10% additional incidence of adverse skeletal changes, cleft palate or any other relevant morphological alteration (BMD<sub>10</sub>). The BMD<sub>10</sub> of each compound was calculated with BMD and PROAST software (Slob, 2002) using dichotomous concentration-response models (quantal data). Among the several models that were fitted, the selection of the best model was determined based on the goodness of fit ( $p$ -value > 0.05). The *in vivo* prenatal developmental toxicity data for the three new azoles were provided by BASF. For the three novel compounds, given the available data, we proceeded with a qualitative *in vivo* potency ranking concept, which was adjusted and applied in our study, including also the known compounds. For implementing this approach of *in vivo* analysis, the profiles of the tested compounds were characterized as potent, moderate and weak or non-potent.

### 3. Results

#### 3.1. Relative potency of azoles causing morphological alterations in rat WEC

All azoles induced some form of developmental toxicity in a concentration-dependent manner in WEC (Fig. 1, Table 2). All newly tested compounds showed statistically significant effects on TMS at concentrations higher than 60  $\mu$ M, except B599, which affected TMS at 20  $\mu$ M (Table 2). Caudal neural tube and somite formation were the most sensitive parameters for all compounds, except PRO. ID<sub>10</sub> concentrations on TMS were calculated for all the tested compounds from Fig. 1, after combining the current and our previous study (Dimopoulou et al., 2017). The decreasing potency ranking of the tested azoles was as follows: B599 > FLU ~ MCZ > KTZ > DFZ ~ B600 > TEB > FEN > TDF > B595 > PRO > PTZ with ID<sub>10</sub>s of 5, 25, 40, 110, 115, 140, 150, 180, 220 and 250  $\mu$ M, respectively.

#### 3.2. Significantly regulated genes across twelve azoles

For studying the effect of the tested azoles on the transcriptome, embryos were exposed for 4 h on GD10 (0–4 h of culture) to the ID<sub>10</sub> concentration of each compound, as calculated from Fig. 1. Somite formation was unaffected directly after all 4-h exposures, indicating the absence of developmental delays at that stage (Fig. 2).

For analysing the gene expression data, we compared each exposure group with the appropriate concurrent vehicle control and we applied the same stringency criteria as mentioned previously ( $p$ -value < 0.001 and FDR of 10%) (Dimopoulou et al., 2017). The combined data

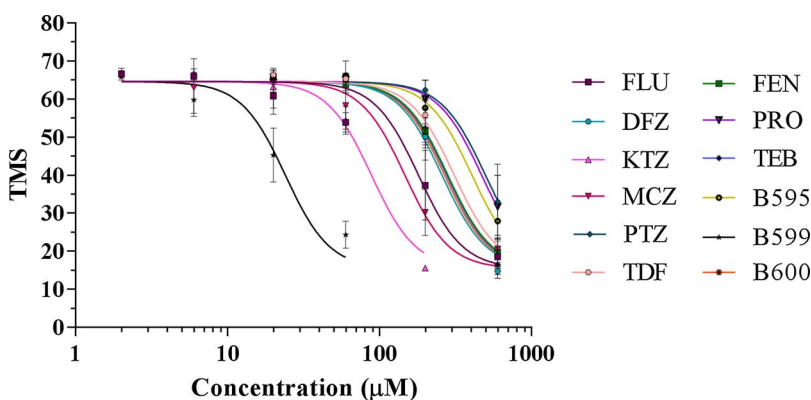


Fig. 1. Total Morphological Score (TMS) concentration-responses of twelve azoles in the rat WEC after 48 h of exposure. Each point represents a mean  $\pm$  SD (N = 8). The curves for the six compounds in the left side list were reproduced from (Dimopoulou et al., 2017).

analysis revealed 53 genes that were statistically significantly regulated by at least one of the twelve azoles. As shown in Fig. 3, embryonic exposure to KTZ and DFZ caused the highest number of statistically significant regulation of genes. On the other hand, MCZ and PTZ did not show statistically significantly regulated genes under the stringency criteria applied.

The hierarchical clustering of the expression data of the 53 genes is illustrated as a heatmap (Fig. 4). Pathway analysis using DAVID revealed enrichment of genes involved in six pathways or processes; RA metabolism, general development, sterol biosynthesis, apoptosis, neural differentiation and vessel formation (Fig. 4, right panel). For some of the genes, an overlap was observed among pathways. For example, *Cyp26a1* appears both in the RA pathway and in the general development pathway.

#### 3.3. Quantitative gene expression changes in the RA and sterol biosynthesis pathways

Within the six functional gene groups that were identified, the RA and sterol biosynthesis pathways were further analysed. As illustrated in Fig. 5, the RA pathway showed a higher magnitude of regulation compared to the sterol biosynthesis pathway in embryos exposed to most compounds, excluding DFZ, MCZ and PTZ. DFZ induced regulation of both pathways to the same extent. MCZ and PTZ revealed a lack of response of both pathways under the significance thresholds applied.

#### 3.4. Gene expression changes observed throughout the sterol biosynthesis pathway

The sterol biosynthesis pathway in mammalian systems consists of a cascade of enzymatic reactions initiated by fatty acid degradation. As in fungi, lanosterol is further converted to intermediate moieties, which are substrates for *Cyp51*, *Msmo1* and *Nsdhl* for synthesizing cholesterol (Fig. 6A).

We numbered the enzymes included on the microarray in the order of appearance in the sterol biosynthesis pathway (Fig. 6A) and plotted their gene expression changes by the different azoles (Fig. 6B). *Msmo1* showed the highest gene expression regulation after exposure to the tested compounds, except for PTZ, TEB and B599 (Fig. 6B). The greatest effect on the regulation of *Msmo1* was observed in rat embryos exposed to DFZ (1.96), KTZ (1.82) and TDF (1.55). The remaining genes were regulated in a relatively similar expression ratio, with the exception of *Dhcr7* in the case of PRO, which reached almost the same level of expression of *Msmo1* (Fig. 6B), at a fold change of 1.5.

#### 3.5. A general comparison of *in vivo* and *in vitro* data

*In vivo* studies on rat embryos, in which the developmental toxic profile of the twelve azoles was tested, were further analysed and the BMD<sub>10</sub> value of each compound was calculated (Table 3). With these



**Table 2**  
Overview of morphological effects of the tested azoles in the rat WEC assay.

Compound	Concentration (µM)	TMS	CRL (mm)	S <sub>48h</sub> – S <sub>0h</sub>	FORE	MID	HIND	CAUD	OTIC	OPTIC	BRAN	MAND-MAX	SOM	HEART
DMSO	0	65.8 ± 10.7	4 ± 0.11	25 ± 0.83	–	–	–	–	–	–	–	–	–	–
FEN	20	65.9 ± 1.74	4.1 ± 0.09	24 ± 0.92	–	–	–	–	–	–	–	–	–	–
	60	63.8 ± 1.62	4.0 ± 0.27	24 ± 1.28	–	–	–	–	–	–	–	–	–	–
	200	51.7 ± 7.71***	3.7 ± 0.19	20 ± 2.00***	–	–	–	**	*	–	*	*	**	–
	600	19.8 ± 3.35****	2.3 ± 0.52***	#	****	****	****	****	****	****	****	****	****	****
PRO	20	65.2 ± 1.71	4.0 ± 0.16	25 ± 0.92	–	–	–	–	–	–	–	–	–	–
	60	64.4 ± 1.75	4.1 ± 0.09	24 ± 0.92	–	–	–	–	–	–	–	–	–	–
	200	60.0 ± 5.04*	3.8 ± 0.18	23 ± 1.13*	–	–	–	–	–	–	*	–	–	–
	600	31.8 ± 8.24****	3.1 ± 0.32***	#	****	****	****	****	****	****	****	**	****	****
TEB	20	65.7 ± 1.07	4.2 ± 0.14	24 ± 0.52	–	–	–	–	–	–	–	–	–	–
	60	63.6 ± 2.03	4.0 ± 0.28	23 ± 0.93	–	–	–	–	–	–	–	–	–	–
	200	52.4 ± 5.22**	3.7 ± 0.16	19 ± 2.00*	–	–	–	**	–	–	*	–	**	–
	600	15.3 ± 20.5****	1.7 ± 0.10*	#	****	****	****	****	****	****	****	****	****	****
B595	60	66.2 ± 0.84	3.9 ± 0.17	24 ± 1.19	–	–	–	–	–	–	–	–	–	–
	200	57.7 ± 4.24*	3.7 ± 0.19*	22 ± 1.93*	–	–	–	*	–	–	–	–	**	–
	600	27.9 ± 12.12***	2.9 ± 0.58****	14 ± 4.96****	****	****	****	****	****	****	****	****	****	****
B599	2	65.9 ± 0.92	4.0 ± 0.19	24 ± 0.00	–	–	–	–	–	–	–	–	–	–
	6	59.8 ± 3.60	4.0 ± 0.14	23 ± 0.71	–	–	–	–	–	–	–	–	–	–
	20	45.3 ± 7.10**	3.7 ± 0.16	18 ± 1.28***	**	–	–	****	**	–	**	–	**	–
	60	24.4 ± 3.57****	2.7 ± 0.23***	12 ± 3.78****	****	****	****	****	****	****	****	****	****	****
B600	60	65.1 ± 1.32	3.9 ± 0.37	24 ± 0.64	–	–	–	–	–	–	–	–	–	–
	200	50.3 ± 1.60*	3.5 ± 0.23*	23 ± 0.92*	–	–	*	**	–	–	*	*	–	*
	600	19.0 ± 3.67****	1.9 ± 0.50****	#	****	****	****	****	****	****	****	****	****	****

Each number represents a mean ± SD (N = 8, Student’s t-test: \*p < 0.05, \*\*p < 0.005, \*\*\*p < 0.0005, \*\*\*\*p < 0.0001). CRL: crown-rump length; S<sub>48h</sub>-S<sub>0h</sub>: number of somites that formed during the culture period of rat WEC; FORE: forebrain; MID: midbrain; HIND: hindbrain; CAUD: caudal neural tube; OTIC: otic system; OPTIC: optic system; BRAN: branchial arches; MAND-MAX: mandibular and maxillary process; SOM: quality of somites and HEART: heart; “#”: could not be measured.

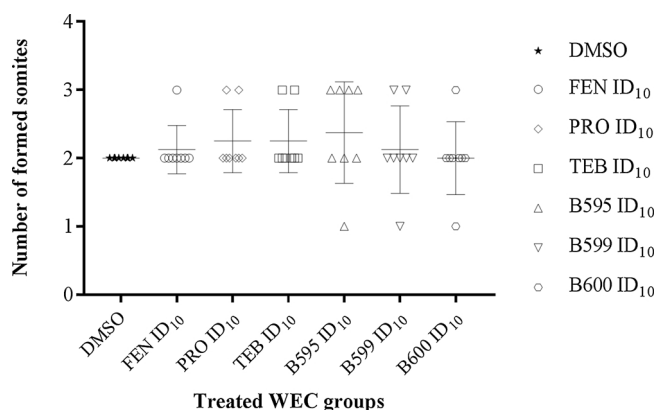


**Fig. 2.** Somitogenesis in rat embryos exposed for 4 h to six azoles at their ID<sub>10</sub> concentration, collected for whole transcriptome analysis. Individual data with mean ± SD are plotted (N = 8 embryos per group).

data, we performed a potency ranking based on the calculated BMD<sub>10</sub> concentration, which was based on an overall assessment of doses-

dependent embryotoxic effects. The BMD<sub>10</sub> was derived based on the most sensitive endpoint, which might differ between compounds. Abnormalities might include skeletal defects, cleft palate, and absence of renal papilla or hydronephrosis. For the three novel compounds B595, B599 and B600, *in vivo* prenatal developmental toxicity data were provided by BASF SE laboratories. The potency ranking of these compounds was qualitatively performed based on limited dose-response information (Li et al., 2016) and resulted in the following order: B599 > B600 > B595. Based on the *in vivo* qualitative and quantitative (where applicable) data, we allocated the twelve tested compounds into one of three developmental toxicity potency groups. The most potent compounds were B599, FLU and KTZ. The moderately embryotoxic compounds *in vivo* were B600, FEN, MCZ, TDF and TEB, while the weak or non-potent compounds were B595, DFZ, PRO and PTZ (Table 3). Table 3 contains also our *in vitro* data of the twelve azoles, including the ID<sub>10</sub> concentrations based on TMS.

Fig. 7 shows a comparison of RA pathway regulation (x-axis), ID<sub>10</sub> in WEC (y-axis) and sterol biosynthesis pathway regulation (z-axis) with *in vivo* potency groups (Table 3, bar colour). B599, FLU and KTZ, the potent developmental toxicants profile both *in vivo* (red bars) and *in vitro* (low ID<sub>10</sub> in the WEC assay), tended to have a more pronounced

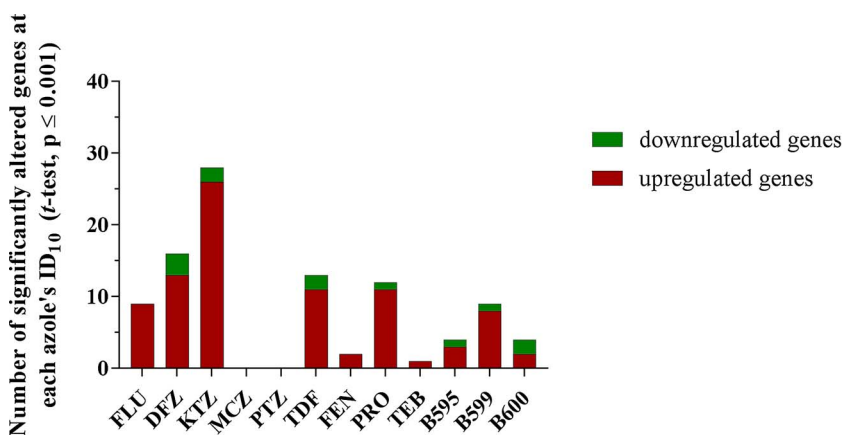


**Fig. 3.** Number of genes statistically significantly regulated by each azole at the ID<sub>10</sub> on TMS among the tested azoles (p-value < 0.001 and FDR 10%).

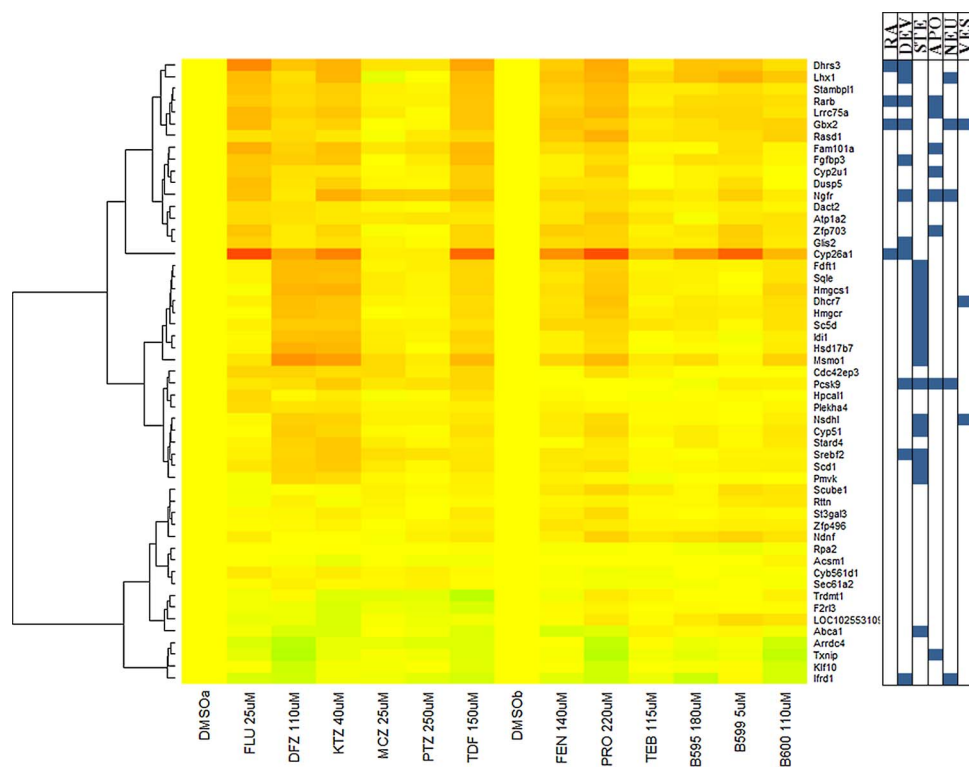


**Fig. 4.** Hierarchical clustering of the average gene expression change in rat WEC by twelve azoles (N = 8, p-value < 0.001 and FDR 10%), with which 53 genes were identified as statistically significantly regulated by at least one of the compounds. Right panel: gene functionality in six pathways: RA (RA), general development (DEV), sterol biosynthesis (STE), apoptosis (APO), neural differentiation (NEU) and vessel formation (VES). Colors indicate changes to vehicle. Red, up-regulation; green, down-regulation; yellow, unchanged. (For interpretation of the references to colour in this figure legend, the reader is referred to the web version of this article.)

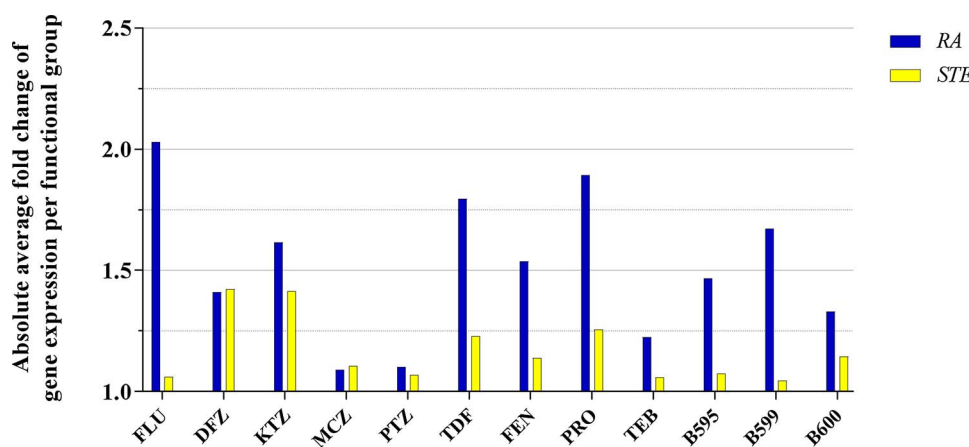


**Fig. 5.** Quantitative gene expression changes, related to the RA and sterol biosynthesis pathways, of twelve azoles in the rat WEC.

effect on regulation of the RA pathway (Fig. 7). The compounds with moderate developmental toxic profile (yellow bars) showed a more limited effect on the RA and sterol biosynthesis pathways. MCZ was classified as a moderate compound in the *in vivo* situation, which was not in agreement with the morphological assessment of embryos in the WEC assay. Additionally, the transcriptomic data revealed an absence of gene-responses in embryos exposed to this azole (Fig. 3). These data were similar to the transcriptome data obtained from embryos exposed to PTZ, which was selected as a non-toxic compound for our study. In contrast, PRO, a weak embryotoxicant *in vivo* and *in vitro*, presented a strong RA-related profile, similar to TDF. DFZ and KTZ conceded a comparable regulation of the sterol biosynthesis pathway, but DFZ did not significantly disturb the RA-related genes. For the remainder of the compounds, we found mixed responses, with a stronger regulation of the RA pathway than of the sterol biosynthesis pathway (Fig. 7).

**4. Discussion**

In the present study, azoles induced concentration dependent

developmental toxic responses in rat WEC, including abnormalities in neural tube closure, formation of the branchial arches and development of the otic cup. Embryos exposed *in vivo* to the same azoles demonstrated commonly observed abnormalities for triazoles, including cleft palate (Tachibana and Monro, 1987) and skeletal abnormalities (Becker et al., 1988; Giknis 1987; Ito et al., 1976; Lochry 1987; Stahl, 1997; Unger et al., 1982), or hydronephrosis (Hoffman et al., 1980) and abnormalities in the urogenital system (Lamontia and Alvarez, 1984). It should be noted that some of these abnormalities are induced *in vivo* at stages beyond the WEC developmental period. The pattern of abnormalities due to either *in vivo* or *in vitro* exposure to azoles is similar to that observed after exposure to RA (Luijten et al., 2010; Robinson et al., 2012c). This observation is supportive of an involvement of the RA pathway in the developmental toxicity of azoles. Comparing *in vitro* ID<sub>10</sub> with the *in vivo* BMD<sub>10</sub> levels (Table 3), we concluded that potency ranking in the WEC was largely similar to the potency ranking in the *in vivo* situation.

We identified 53 genes statistically significantly regulated (ANOVA, p-value < 0.001, FDR 10%) by at least one of the compounds, which

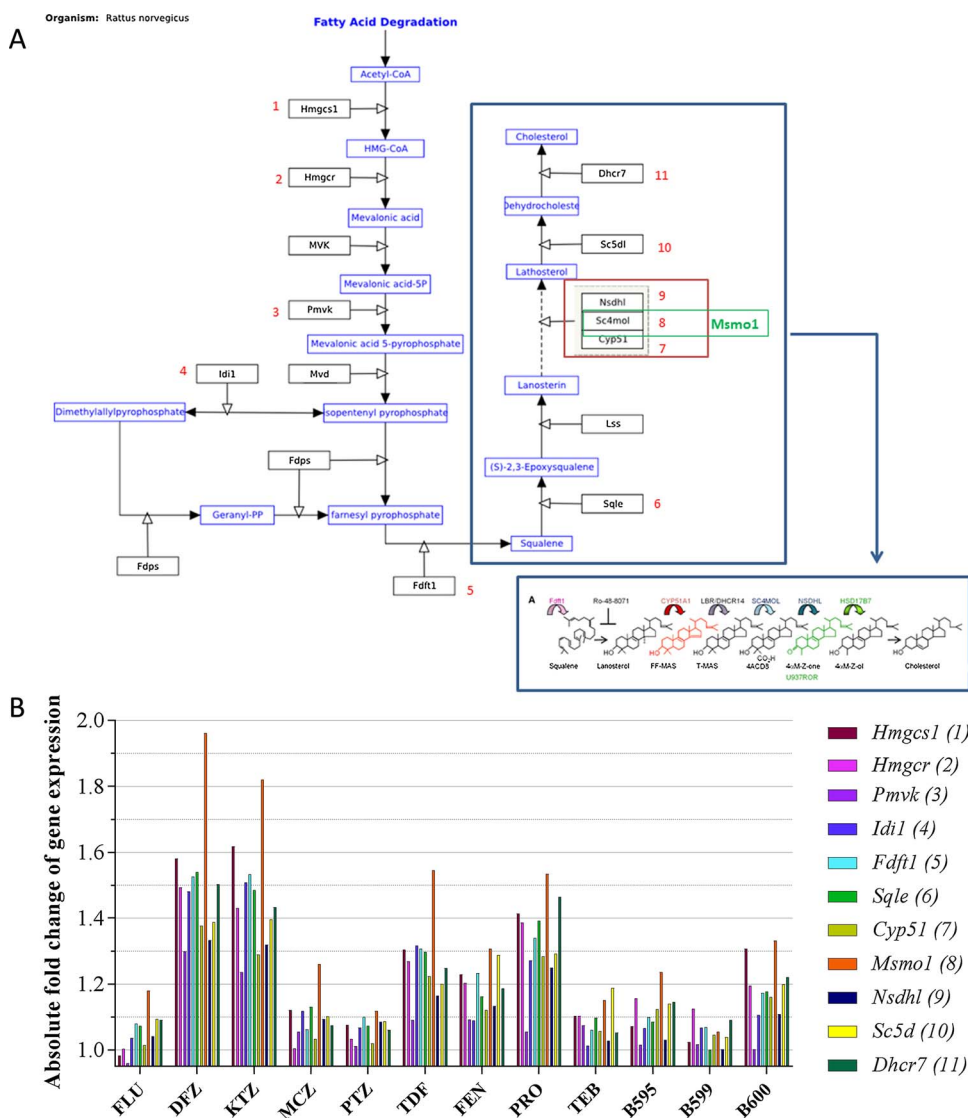


**Fig. 6.** A. The sterol biosynthesis pathway in the *Rattus norvegicus*, including the main intermediate moieties and the contributing enzymes adapted from [www.wikipathways.org](http://www.wikipathways.org) (Kutmon et al., 2016) and (Santori et al., 2015). B. The quantitative regulation of the genes that participate in the sterol biosynthesis pathway in rat WEC exposed to twelve azoles.

**Table 3**  
Overview of *in vivo* and *in vitro* developmental toxicity data of twelve azoles.

Compound	<i>in vitro</i> WEC		<i>in vivo</i>	Potency Group
	ID <sub>10</sub> (μM)	BMD <sub>10</sub> (μmol/kg)		
B599	5	–	–	Potent
FLU	25	9.1 (Lamontia and Alvarez, 1984)	–	Potent
MCZ	25	258.3 (Ito et al., 1976)	–	Moderate
KTZ	40	20.1 (Tachibana and Monro, 1987)	–	Potent
B600	110	–	–	Moderate
DFZ	110	596.5 (Lochry, 1987)	–	Weak
TEB	115	275.8 (Becker et al., 1988)	–	Moderate
FEN	140	88.5 (Hoffman et al., 1980)	–	Moderate
TDF	150	91.5 (Unger et al., 1982)	–	Moderate
B595	180	–	–	Weak
PRO	220	386.7 (Giknis, 1987)	–	Weak
PTZ	250	917.8 (Stahl, 1997)	–	Weak

were further categorized into six functional gene-groups. We further analysed the responses of genes associated with the sterol biosynthesis and RA pathways, due to their crucial role for determining the fungicidal mode of action (sterol biosynthesis pathway) and the embryotoxic potency (RA pathway) of the tested compounds.

Among the regulated sterol biosynthesis related genes, *Msmo1* showed the highest increase in expression, after embryonic exposure to

KTZ and DFZ, as well as TDF and PRO. Despite the fact that mammalian systems are less sensitive than fungal systems to azoles (Trosken et al., 2006), the expression of sterol related genes in both biological systems determines azoles' fungicidal activity. The observed significant induction of *Msmo1* (or its synonym, *Sc4mol*) was also identified in previous studies in the rat WEC (Dimopoulou et al., 2017; Robinson et al., 2012b), as well as in the zebrafish test (ZET) (Hermsen et al., 2012) and Embryonic Stem Cell Test (EST) (van Dartel et al., 2011). Additionally, considering that the expression pattern of all the individual sterol related genes was constant among the tested compounds (Fig. 6B), we suggest that *Msmo1* could be a more sensitive biomarker compared to the already characterized biomarker *Cyp51* (Marotta and Tiboni, 2010) for studying the fungicidal activity. However, for concluding about the extent of each gene's specific importance in the sterol biosynthesis pathway, studies on the level of the metabolome are needed. *Msmo1* is involved in an oxidation-reduction process, while it is also associated with malformations, such as microcephaly and congenital cataract, which could be linked with its extra role in the central nervous system development (CNS), and especially in the midbrain neurogenesis (He et al., 2011). Pinto et al. (Pinto et al., 2016) described that *Msmo1* transcription is activated by the liver X receptors (LXR), which are binding to the retinoid X receptors (RXR), a connection that could be further associated with RA. Additionally, *Srebp* transcriptional factors regulate the cholesterol biosynthesis pathway in mammalian systems,

## 12 azoles: RA pathway vs Sterol biosynthesis pathway

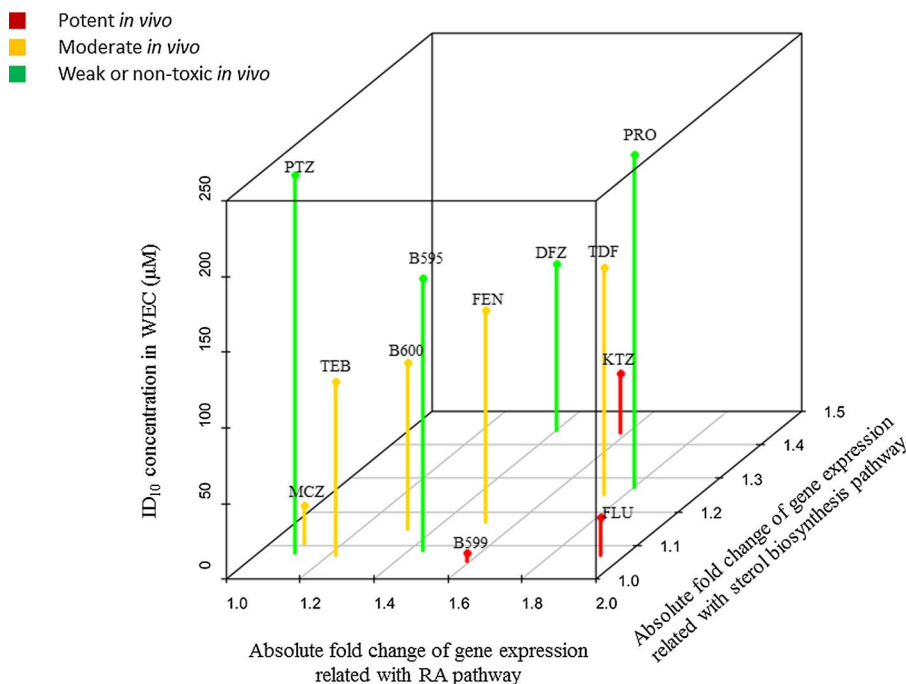


Fig. 7. Correlation of *in vivo* and *in vitro* in the rat WEC data for twelve tested azoles. Bars with red, yellow and green colour indicate in a qualitative way the potent, moderate and weak or non-toxic *in vivo* profile of these azoles. The length of the bars represents the *in vitro* ID<sub>10</sub> concentration (y-axis). (For interpretation of the references to colour in this figure legend, the reader is referred to the web version of this article.)

via interacting with the binding sites of *Hmgcr* and *Fdft1* in the mevalonate arm in the beginning of the pathway (Mazein et al., 2013). *Srebp* interacts directly with LXR and therefore may indirectly regulate genes in the sterol biosynthesis pathway (Horton, 2002; Pinto et al., 2016).

Additionally, we observed that the potent *in vivo* and *in vitro* embryotoxicants, as well as the moderate TDF and the weak PRO, altered the expression of RA-related genes in a similar manner. The commonly highest upregulated gene was *Cyp26a1*, which is upregulated for metabolizing excess level of RA (Rhinn and Dollé, 2012). Therefore, we suggest that the overexpression of the RA pathway could be the underlying mechanism of induced developmental toxicity of azoles in the rat WEC. Consequently, the application of RA-related biomarkers is valuable for distinguishing highly potent embryotoxicants within the same class of chemicals.

MCZ, a compound with potent *in vitro* and moderate *in vivo* embryotoxic potency, lacked a statistically significant response on the level of transcriptome in our combined analysis. This suggests that transcriptomics may not be the optimal method to detect the embryotoxic mode of action of MCZ. Apoptosis, an additionally identified functional gene group, was extensively regulated by the azoles that showed the highest response of RA-related genes. Interestingly, similar to the strong *in vitro* embryotoxicants FLU, KTZ and B599, MCZ did show enhanced expression of *Ngfr*, an apoptosis related gene (Fig. 4). *Ngfr* is associated with neuron differentiation in the brain region (Do et al., 2016), while it has been also suggested to be mediator for thyroid hormone activation (Porterfield, 2000) and a negative regulator of angiogenesis (Parsi et al., 2012). Another apoptosis related strong effect was identified on the expression of *Fam101a*, which is localized in the midbrain and forebrain of 5-somite stage embryos (Hirano et al., 2005; Mizuhashi et al., 2014), while it is involved in the bone maturation and interacts with RA (NCBI, 2013). Furthermore, *Txnip*, a general biomarker of stress responses, is related with the dysregulation of cell division (Dunn et al., 2010; Patwari et al., 2006). The similarity of expression among genes of RA and apoptosis pathways could support our hypothesis that RA related responses are directly linked to developmental toxic responses and, therefore, could justify the consequent embryotoxicity of the corresponding azoles.

Moreover, *Lhx1*, the most pronounced expressed gene among the

neural differentiation related genes, was remarkably affected in WEC exposed to B599, FLU, KTZ and TDF, which are among the most potent compounds. *Lhx1* has been also suggested to be indirectly associated with RA and RA-related morphological alterations. It is localized in the brain and has been shown to interact with development related genes and transcriptional factors (Furuyama et al., 1994), such as the *Hox* and *Pax* genes, and therefore, it could be indirectly correlated with the activation of the *Gata* and *Wnt* signalling pathways (Costantini and Kopan, 2010; Hevner et al., 2002; Pratt et al., 2000). Karavanov et al. (Karavanov et al., 1998) have also described its additional role in the kidney development during embryonic development and in later stages for maintaining the function of the ureteric bud.

Embryos exposed to azoles with high ID<sub>10</sub> concentrations disclosed a notable downregulation of a set of genes, which could explain the sensitivity of the WEC system compared to the *in vivo* screening in ranking DFZ and PRO. The highest regulation of *Ifrd1*, which participates in neuron differentiation and general development pathways (Fig. 4), could be associated with cellular stress in multicellular organisms according to Zhao et al. (Zhao et al., 2010). In those embryos, we also observed a significant accompanied downregulation of both *Arrdc4*, a protein that regulates the ubiquitin-protein transferase activity (Mackenzie et al., 2016), and *Txnip* (Fig. 4). *Txnip* is a member of the alpha arrestin protein family (to which *Arrdc4* belongs too), however the exact mechanism of collaboration of these two genes has not been elucidated yet (Fishilevich et al., 2017).

To summarize, we investigated the potency ranking of twelve azoles in the rat WEC, the vast majority of which was in line with the *in vivo* potency ranking. We also studied the toxicological and fungicidal mode of action of the selected compounds on the level of transcriptome using the set of biomarkers that has been previously selected (Dimopoulou et al., 2017). We concluded that the most potent embryotoxicants, both *in vivo* and *in vitro*, revealed an overexpression of genes that participated in RA related pathways, and were associated with apoptosis and stress responses. Moreover, we identified responses of genes that participated in the sterol biosynthesis pathway and, therefore, related to the fungicidal mode of action. We found that *Msmo1* was a more sensitive biomarker for screening the functional efficacy of azoles compared to *Cyp51*, which could improve the *in vitro* assessment of existing



and future antifungal chemicals.

## Conflict of interest

None

## Funding information

This work was supported by a collaborative project between Wageningen University (grant number 6153511466), RIVM and BASF SE.

## References

- Augustine-Rauch, K., Zhang, C.X., Panzica-Kelly, J.M., 2010. In vitro developmental toxicology assays: a review of the state of the science of rodent and zebrafish whole embryo culture and embryonic stem cell assays. *Birth Defects Res. C Embryo Today* 90, 87–98.
- Becker, H., Vogel, W. & Terrier, C. 1988. Embryotoxicity study (including teratogenicity) with HWG 1608 technical in rat. Unpublished report Ref. No. R 4451, prepared by Research & Consulting Co. AG (RCC), Itingen, Switzerland. Submitted to WHO by Bayern AG, Leverkusen, Germany.
- Brown, N.A., Fabro, S., 1981. Quantitation of rat embryonic development in vitro: a morphological scoring system. *Teratology* 24, 65–78.
- Costantini, F., Kopan, R., 2010. Patterning a complex organ: branching morphogenesis and nephron segmentation in kidney development. *Dev. Cell* 18, 698–712.
- Cunningham, T.J., Duester, G., 2015. Mechanisms of retinoic acid signalling and its roles in organ and limb development. *Nat. Rev. Mol. Cell Biol.* 16, 110–123.
- Dai, M., Wang, P., Boyd, A.D., Kostov, G., Athey, B., Jones, E.G., Bunney, W.E., Myers, R.M., Speed, T.P., Akil, H., Watson, S.J., Meng, F., 2005. Evolving gene/transcript definitions significantly alter the interpretation of GeneChip data. *Nucleic Acids Res.* 33, e175.
- Daston, G.P., Naciff, J.M., 2010. Predicting developmental toxicity through toxicogenomics. *Birth Defects Res. C Embryo Today* 90, 110–117.
- de Jong, E., Barenys, M., Hermsen, S.A., Verhoef, A., Ossendorp, B.C., Bessems, J.G., Piersma, A.H., 2011. Comparison of the mouse Embryonic Stem cell Test, the rat Whole Embryo Culture and the Zebrafish Embryotoxicity Test as alternative methods for developmental toxicity testing of six 1,2,4-triazoles. *Toxicol. Appl. Pharmacol.* 253, 103–111.
- Dimopoulou, M., Verhoef, A., van Ravenzwaay, B., Rietjens, I.M., Piersma, A.H., 2016. Flusilazole induces spatio-temporal expression patterns of retinoic acid-, differentiation- and sterol biosynthesis-related genes in the rat Whole Embryo Culture. *Reprod. Toxicol. (Elmsford N.Y.)* 64, 77–85.
- Dimopoulou, M., Verhoef, A., Pennings, J.L.A., van Ravenzwaay, B., Rietjens, I., Piersma, A.H., 2017. Embryotoxic and pharmacologic potency ranking of six azoles in the rat whole embryo culture by morphological and transcriptomic analysis. *Toxicol. Appl. Pharmacol.* 322, 15–26.
- Do, H.T., Bruelle, C., Pham, D.D., Jauhainen, M., Eriksson, O., Korhonen, L.T., Lindholm, D., 2016. Nerve growth factor (NGF) and pro-NGF increase low-density lipoprotein (LDL) receptors in neuronal cells partly by different mechanisms: role of LDL in neurite outgrowth. *J. Neurochem.* 136, 306–315.
- Dunn, L.L., Buckle, A.M., Cooke, J.P., Ng, M.K.C., 2010. The emerging role of the thioredoxin system in angiogenesis. *Arterioscler. Thromb. Vasc. Biol.* 30, 2089–2098.
- Eijssen, L.M., Jaillard, M., Adriaens, M.E., Gaj, S., de Groot, P.J., Muller, M., Evelo, C.T., 2013. User-friendly solutions for microarray quality control and pre-processing on ArrayAnalysis.org. *Nucleic Acids Res.* 41, W71–76.
- Fishilevich, S., Nudel, R., Rappaport, N., Hadar, R., Plaschkes, I., Iny Stein, T., Rosen, N., Kohn, A., Twik, M., Safran, M., Lancet, D., Cohen, D., 2017. GeneHancer: genome-wide integration of enhancers and target genes in GeneCards. *Database* 2017 bax028–bax028.
- Furuyama, T., Inagaki, S., Iwahashi, Y., Takagi, H., 1994. Distribution of Rlim, an LIM homeodomain gene, in the rat brain. *Neurosci. Lett.* 170, 266–268.
- Giknis, M.L.A., 1987. A Teratology (segment II) Study in Rats. Unpublished Report No.: 86004 from Ciba-Geigy Pharmaceutical Division, New Jersey. Submitted to WHO by Ciba-Geigy Ltd., Basle, Switzerland.
- He, M., Kratz, L.E., Michel, J.J., Vallejo, A.N., Ferris, L., Kelley, R.I., Hoover, J.J., Jukic, D., Gibson, K.M., Wolfe, L.A., Ramachandran, D., Zwick, M.E., Vockley, J., 2011. Mutations in the human SC4MOL gene encoding a methyl sterol oxidase cause psoriasisform dermatitis, microcephaly, and developmental delay. *J. Clin. Invest.* 121, 976–984.
- Hermsen, S.A., Pronk, T.E., van den Brandhof, E.J., van der Ven, L.T., Piersma, A.H., 2012. Triazole-induced gene expression changes in the zebrafish embryo. *Reprod. Toxicol. (Elmsford, N.Y.)* 34, 216–224.
- Hevner, R.F., Miyashita-Lin, E., Rubenstein, J.L., 2002. Cortical and thalamic axon pathfinding defects in Tbr1, Gbx2, and Pax6 mutant mice: evidence that cortical and thalamic axons interact and guide each other. *J. Comp. Neurol.* 447, 8–17.
- Hirano, M., Murata, T., Furushima, K., Kiyonari, H., Nakamura, M., Suda, Y., Aizawa, S., 2005. cfm is a novel gene uniquely expressed in developing forebrain and midbrain: but its null mutant exhibits no obvious phenotype. *Gene Expr. Patterns* 5, 439–444.
- Hoffman, D.G., Owen, N.V., Adams, E.R., 1980. A Teratology Study with EL-222 in the Rat. Unpublished Report No. R06279 Form Lilly Research Laboratories, USA.
- Submitted to WHO by DowElanco Europe, Wantage, Oxon, United Kingdom.
- Horton, J.D., 2002. Sterol regulatory element-binding proteins: transcriptional activators of lipid synthesis. *Biochem. Soc. Trans.* 30, 1091–1095.
- Huang da, W., Sherman, B.T., Lempicki, R.A., 2009. Systematic and integrative analysis of large gene lists using DAVID bioinformatics resources. *Nat. Protoc.* 4, 44–57.
- Irizarry, R.A., Hobbs, B., Collin, F., Beazer-Barclay, Y.D., Antonellis, K.J., Scherf, U., Speed, T.P., 2003. Exploration, normalization, and summaries of high density oligonucleotide array probe level data. *Biostatistics (Oxford England)* 4, 249–264.
- Ito, C., Shibutani, Y., Inoue, K., Nakano, K., Ohnishi, H., 1976. Toxicological studies of miconazole (II) teratological studies of miconazole in rats. *IYAKUHIN KENKYU* 7, 367–376.
- Karavanov, A.A., Karavanova, I., Perantoni, A., Dawid, I.B., 1998. Expression pattern of the rat Lim-1 homeobox gene suggests a dual role during kidney development. *Int. J. Dev. Biol.* 42, 61–66.
- Kutmon, M., Riutta, A., Nunes, N., Hanspers, K., Willighagen Egon, L., Bohler, A., Mélius, J., Waagmeester, A., Sinha Sravanthi, R., Miller, R., Coort, S.L., Cirillo, E., Smeets, B., Evelo Chris, T., Pico, A.R., 2016. WikiPathways: capturing the full diversity of pathway knowledge. *Nucleic Acids Res.* 44, D488–D494.
- Lamontia CL, S.R., Alvarez L. 1984. Embryo-fetal toxicity and teratogenicity study of INH-6573-39 by gavage in the rat. Unpublished reports No. HLR 444-83 and HLR 142-84 from Haskell Laboratory for Toxicology and Industrial Medicine, Wilmington, Delaware, USA. Submitted to WHO by E.I. du Pont de Nemours & Co., Inc., Wilmington, Delaware, USA. Summarized in JMPR Monograph—Flusilazole, Pesticide residues in food: 1995 evaluations Part II Toxicological & EnvironmentEnvironment. <http://www.inchem.org/documents/jmpr/jmpmono/v95pr08.htm>.
- Li, H., Flick, B., Rietjens, I.M., Louise, J., Schneider, S., van Ravenzwaay, B., 2016. Extended evaluation on the ES-D3 cell differentiation assay combined with the BeWo transport model, to predict relative developmental toxicity of triazole compounds. *Arch. Toxicol.* 90, 1225–1237.
- Lochry, E.A. 1987. Developmental toxicity study of CGA-169374 technical (FL-851406) administered orally via gavage to Crl:COBS CD (SD) BR presumed pregnant rats. Unpublished report No. 203-005 from Novartis Crop Protection AG., Basel, Switzerland and Argus Research Lab. Inc., Horsham, USA, Submitted to WHO by SYgenta Crop Protection AG, Basel, Switzerland. [http://apps.who.int/iris/bitstream/10665/44064/1/9789241665230\\_eng.pdf?ua=1](http://apps.who.int/iris/bitstream/10665/44064/1/9789241665230_eng.pdf?ua=1).
- Luijten, M., van Beelen, V.A., Verhoef, A., Renkens, M.F., van Herwijnen, M.H., Westerman, A., van Schooten, F.J., Pennings, J.L., Piersma, A.H., 2010. Transcriptomics analysis of retinoic acid embryotoxicity in rat postimplantation whole embryo culture. *Reprod. Toxicol. (Elmsford, N.Y.)* 30, 333–340.
- Mackenzie, K., Foot, N.J., Anand, S., Dalton, H.E., Chaudhary, N., Collins, B.M., Mathivanan, S., Kumar, S., 2016. Regulation of the divalent metal ion transporter via membrane budding. *Cell Discov.* 2, 16011.
- Marotta, F., Tiboni, G.M., 2010. Molecular aspects of azoles-induced teratogenesis. *Expert Opin. Drug Metab. Toxicol.* 6, 461–482.
- Mazein, A., Watterson, S., Hsieh, W.Y., Griffiths, W.J., Ghazal, P., 2013. A comprehensive machine-readable view of the mammalian cholesterol biosynthesis pathway. *Biochem. Pharmacol.* 86, 56–66.
- Menegola, E., Brocchia, M.L., Di Renzo, F., Giavini, E., 2006. Dysmorphic effects of some fungicides derived from the imidazole on rat embryos cultured in vitro. *Reprod. Toxicol. (Elmsford, N.Y.)* 21, 74–82.
- Mizuhashi, K., Kanamoto, T., Moriishi, T., Muranishi, Y., Miyazaki, T., Terada, K., Omori, Y., Ito, M., Komori, T., Furukawa, T., 2014. Filamin-interacting proteins, Cfm1 and Cfm2, are essential for the formation of cartilaginous skeletal elements. *Hum. Mol. Genet.* 23, 2953–2967.
- NCBI, 2013. Database resources of the national center for biotechnology information. *Nucleic Acids Res.* 41, D8–D20.
- New, D.A., Coppola, P.T., Cockroft, D.L., 1976. Comparison of growth in vitro and in vivo of post-implantation rat embryos. *J. Embryol. Exp. Morphol.* 36, 133–144.
- Parsi, S., Soltani, B.M., Hosseini, E., Tousi, S.E., Mowla, S.J., 2012. Experimental verification of a predicted intronic MicroRNA in human NGFR gene with a potential proapoptotic function. *PLoS One* 7, e35561.
- Patwari, P., Higgins, L.J., Chutkow, W.A., Yoshioka, J., Lee, R.T., 2006. The interaction of thioredoxin with Txnip. Evidence for formation of a mixed disulfide by disulfide exchange. *J. Biol. Chem.* 281, 21884–21891.
- Piersma, A.H., Hessel, E.V., Staal, Y.C., 2017. Retinoic acid in developmental toxicology: teratogen, morphogen and biomarker. *Reprod. Toxicol. (Elmsford, N.Y.)* 72, 53–61.
- Piersma, A.H., 2004. Validation of alternative methods for developmental toxicity testing. *Toxicol. Lett.* 149, 147–153.
- Piersma, A.H., 2006. Alternative methods for developmental toxicity testing. *Basic Clin. Pharmacol. Toxicol.* 98, 427–431.
- Pinto, C.L., Kalasekar, S.M., McCollum, C.W., Riu, A., Jonsson, P., Lopez, J., Swindell, E.C., Bouhlatouf, A., Balaguer, P., Bondesson, M., Gustafsson, J.A., 2016. Lxr regulates lipid metabolic and visual perception pathways during zebrafish development. *Mol. Cell. Endocrinol.* 419, 29–43.
- Porterfield, S.P., 2000. Thyroidal dysfunction and environmental chemicals: potential impact on brain development. *Environ. Health Perspect.* 108, 433–438.
- Pratt, T., Vitalis, T., Warren, N., Edgar, J.M., Mason, J.O., Price, D.J., 2000. A role for Pax6 in the normal development of dorsal thalamus and its cortical connections. *Development* 127, 5167–5178.
- Rhinn, M., Dollé, P., 2012. Retinoic acid signalling during development. *Development* 139, 843–858.
- Robinson, J.F., van Beelen, V.A., Verhoef, A., Renkens, M.F., Luijten, M., van Herwijnen, M.H., Westerman, A., Pennings, J.L., Piersma, A.H., 2010. Embryotoxicant-specific transcriptomic responses in rat postimplantation whole-embryo culture. *Toxicol. Sci.* 118, 675–685.

- Robinson, J.F., Pennings, J.L., Piersma, A.H., 2012a. A review of toxicogenomic approaches in developmental toxicology. *Methods Mol. Biol. (Clifton, N.J.)* 889, 347–371.
- Robinson, J.F., Tonk, E.C., Verhoef, A., Piersma, A.H., 2012b. Triazole induced concentration-related gene signatures in rat whole embryo culture. *Reprod. Toxicol. (Elmsford, N.Y.)* 34, 275–283.
- Robinson, J.F., Verhoef, A., Pennings, J.L., Pronk, T.E., Piersma, A.H., 2012c. A comparison of gene expression responses in rat whole embryo culture and in vivo: time-dependent retinoic acid-induced teratogenic response. *Toxicol. Sci.* 126, 242–254.
- Robinson, J.F., Verhoef, A., Piersma, A.H., 2012d. Transcriptomic analysis of neurulation and early organogenesis in rat embryos: an in vivo and ex vivo comparison. *Toxicol. Sci.* 126, 255–266.
- Santori, F.R., Huang, P., van de Pavert, S.A., Douglass Jr., E.F., Leaver, D.J., Haubrich, B.A., Keber, R., Lorbek, G., Konijn, T., Rosales, B.N., Rozman, D., Horvat, S., Rahier, A., Mebius, R.E., Rastinejad, F., Nes, W.D., Littman, D.R., 2015. Identification of natural RORgamma ligands that regulate the development of lymphoid cells. *Cell Metab.* 21, 286–297.
- Slob, W., 2002. Dose-response modeling of continuous endpoints. *Toxicol. Sci.* 66, 298–312.
- Stahl, B. 1997. JAU 6476 – Developmental toxicity study in rats after oral administration. Unpublished report No. M-012279-01-1 from Bayer AG, Wuppertal, Germany. Submitted to WHO by Bayer CropScience AG, Germany. [https://www.google.nl/url?sa=t&rct=j&q=&esrc=s&source=web&cd=2&ved=0ahUKEwjNcX5-HPAhWDrxoKHebSDzYQFggghMAE&url=http%3A%2F%2Fapps.who.int%2Fpesticide-residues-jmpr-database%2Fdocument%2F110&usg=AFQjCNGpjQOE2xfb0QbWpWwA5-avbrC8kQ&sig2=ZFM7G3fgK4EdIA0e\\_zX0hQ&cad=rja](https://www.google.nl/url?sa=t&rct=j&q=&esrc=s&source=web&cd=2&ved=0ahUKEwjNcX5-HPAhWDrxoKHebSDzYQFggghMAE&url=http%3A%2F%2Fapps.who.int%2Fpesticide-residues-jmpr-database%2Fdocument%2F110&usg=AFQjCNGpjQOE2xfb0QbWpWwA5-avbrC8kQ&sig2=ZFM7G3fgK4EdIA0e_zX0hQ&cad=rja).
- Tachibana, M.N.Y., Monro, A.M., 1987. Toxicology of fluconazole in experimental animals. In: Fromtling, R.A. (Ed.), *Recent Trends in the Discovery, Development, and Evaluation of Antifungal Agents*. JR Prous, Barcelona, pp. 93–102.
- Tonk, E.C.M., Pennings, J.L.A., Piersma, A.H., 2015. An adverse outcome pathway framework for neural tube and axial defects mediated by modulation of retinoic acid homeostasis. *Reprod. Toxicol.* 55, 104–113.
- Trosken, E.R., Adamska, M., Arand, M., Zarn, J.A., Patten, C., Volkel, W., Lutz, W.K., 2006. Comparison of lanosterol-14 alpha-demethylase (CYP51) of human and *Candida albicans* for inhibition by different antifungal azoles. *Toxicology* 228, 24–32.
- Unger, T.M., Van Goethem, D. & Shellenberger. 1982. A teratological evaluation of Bayleton in mated female rats. Midwest Research Institute, Report No. 324 to Mobay Chemical Corporation Agricultural Chemical Division submitted to WHO by Bayer AG. (Unpublished), <http://www.inchem.org/documents/jmpr/jmpmono/v83pr39.htm>.
- van Dartel, D.A., Pennings, J.L., de la Fonteyne, L.J., Brauers, K.J., Claessen, S., van Delft, J.H., Kleinjans, J.C., Piersma, A.H., 2011. Concentration-dependent gene expression responses to flusilazole in embryonic stem cell differentiation cultures. *Toxicol. Appl. Pharmacol.* 251, 110–118.
- van der Jagt K., M.S., Tørsløv J. & de Bruijn J. 2004. Alternative approaches can reduce the use of test animals under REACH EUROPEAN COMMISSION DIRECTORATE GENERAL JRC JOINT RESEARCH CENTRE Institute for Health and Consumer Protection, <http://home.kpn.nl/reach/downloads/reducingtheuseoftestanimalsunderreachihcprepor.pdf>.
- Zhao, C., Datta, S., Mandal, P., Xu, S., Hamilton, T., 2010. Stress-sensitive regulation of IFRD1 mRNA decay is mediated by an upstream open reading frame. *J. Biol. Chem.* 285, 8552–8562.